PERFORMANCE BOUND FOR TIME DELAY AND AMPLITUDE ESTIMATION FROM LOW RATE SAMPLES OF PULSE TRAINS

Ciprian R. Comsa [*,†], *Alexander M. Haimovich* [†]

[*] Telecommunications Dept, "Gheorghe Asachi" Technical University of Iasi, Romania
[†] ECE Dept, New Jersey Institute of Technology, USA

ABSTRACT

The problem considered is estimating the time delays and amplitudes of a train of pulses of known shape. It was recently shown that in the absence of noise, if the pulses are short relative to the interval separating them, the stream of pulses can be sampled at rates lower than the Nyquist rate without any loss of information. This paper investigates the performance of time delay and amplitude estimation from samples taken at low (sub-Nyquist) rates when the stream of pulses is affected by additive white Gaussian noise. To this end, the Cramér-Rao bound (CRB) is developed. For a particular setup, the CRB for time delay estimation is inverse proportional to the cube of the sampling rate, while the CRB for amplitude estimation is inverse proportional to the sampling rate. Numerical simulations confirm this result.

Index Terms — Cramér-Rao bound, time delay and amplitude estimation, low rate sampling, pulse train

1. INTRODUCTION

In many applications, signals can be uniquely described by a small number of parameters. For example, in radar and wireless communications signal can be constituted of a stream of short pulses of known shape, stream that is defined by the time delays and amplitudes of the pulses. Estimation of these parameters is the subject of this work. Time delay estimation and amplitude estimation are conventionally performed from samples taken at rates higher than the Nyquist rate, which is twice the signal's bandwidth. This approach is required when the only knowledge on the signal is that it is bandlimited. Other priors on signal structure can lead to more efficient sampling. An interesting class of structured signals was considered in [1], where the signals have a finite number of degrees of freedom per unit time. These signals were termed to have finite rate of innovation (FRI). A special case of FRI signals consists of a stream of K pulses of known shape per time interval T. For such a stream, any of its segments of length T is uniquely determined by no more than $2K$ parameters, i.e., K time delays and K amplitudes. It is then said that the signal's local rate of innovation is finite and equals $2K/T$.

For streams of pulses of short duration relative to the reference interval T, standard sampling methods require very high sampling rates. However, the rate of innovation per interval T is much smaller than the number of samples taken at the Nyquist rate. This observation was exploited to set the grounds for sampling at rates lower than the Nyquist rate. To this end, a mechanism to sample at low rates streams of Diracs can be found in [1], and the references therein. A scheme for recovering the original stream from the samples was also proposed. More recent work, [2, 3], generalizes the approach to sampling at low rates streams of pulses of known arbitrary shape, rather than just Diracs, by considering a multichannel sampling setup. Although the proposed multichannel sampling scheme allows perfect recovery of the original signal from its noiseless samples, it was found in [4] that in the presence of noise the performance of the signal recovery from low rate samples deteriorates significantly relative to the signal recovery from samples taken at the Nyquist rate. However, with low rate sampling, increasing the sampling rate above the rate of innovation brings substantial performance improvement.

This work considers low rate sampling of streams of pulses as in [2, 3], but rather than recover the signal itself, the goal is to estimate specific signal parameters, specifically, delay and amplitude. The signal recovery in [2, 3] is equivalent to estimating all the unknown signal parameters, e.g., time delays and corresponding amplitudes. By contrast, estimation of individual parameters may be performed independently, e.g., delay estimation does not require the estimation of amplitudes, and thus its performance may vary with system parameters differently than that of signal recovery.

The paper is organized as follows: Section 2 provides the system model for a multichannel sampling scheme. In Section 3, CRB expressions are developed for TDE and amplitude estimation. Discussion of our results vis-à-vis other work is included. Section 4 contains numerical results, and conclusions wrap up the paper.

2. SYSTEM MODEL

The problem considered is estimation of a vector $\boldsymbol{\theta}$ that parameterizes a FRI segment $x(t)$ of length T_0 from samples taken at low rates from a noisy observation $y(t)$. To give practical relevance to the problem considered, $x(t)$ is viewed as the product of transmitting a signal $x_T(t)$ through a multipath channel $h(\tau,t)=\sum_{k=1}^{K}\alpha_k\delta(t-\tau_k)$, where α_k are the complex valued amplitudes and τ_k the time delays associated with each propagation path. The transmitted signal $x_T(t)$ consists of a train of pulses. That is, a pulse of known shape $g(t)$ is emitted periodically at a constant rate $1/T$, after being modulated by some arbitrary, known sequence $x_M[n]$. Vector $\boldsymbol{\theta}$ contains then the time delays and amplitudes as the unknowns that parameterize the signal $x(t)$. It is assumed that $T_0 \gg T > \tau_k$, for any $k \in \{1,\dots,K\}$. Also, the multipath channel is assumed time invariant. Thus, the amplitudes α_k do not change from one interval $\mathrm{I}_n=[(n-1)T,nT]$ to another. Additionally, the received signal is shift invariant, i.e., the time delays also do not change from one interval I_n to another, with respect to the beginning of each interval. The received signal is then a complex valued, noisy semi-periodic train of pulses:

$$y(t)=\sum_{n=1}^{N}\sum_{k=1}^{K}a_k[n]\,g(t-\tau_k-nT)+\eta(t), \qquad (1)$$

where $a_k[n]=\alpha_k x_M[n]$ and $N=T_0/T$. The signal is defined by K time delays τ_k and by NK amplitudes $a_k[n]$. However, any segment of $x(t)$ of length T is defined by only K time delays and K amplitudes. Moreover, with knowledge of the sequence $\{x_M[n]\}$, the whole observed signal $x(t)$, of length T_0, is defined by K time delays τ_k and K amplitudes α_k. Thus signal $x(t)$ is FRI.

The received signal is affected by complex valued additive white Gaussian noise (AWGN), $\eta(t)$, of power spectral density (PSD) $\bar{\Phi}_\eta$. For later use, let $\sigma_\eta^2=\bar{\Phi}_\eta/T$ denote the power of the noise after passing through an ideal low pass filter of cut-off frequency $1/2T$.

The system model for the problem considered is depicted in Fig. 1a. The continuous-time signal $y(t)$ is passed through a *Sampling* block to obtain the set of samples $\boldsymbol{c}$. Based on samples $\boldsymbol{c}$, an estimate of $\boldsymbol{\theta}$ is obtained with the *Estimation* block. For the *Sampling* block a multichannel structure is considered. With a multichannel sampling setup the signal $y(t)$ is convolved with P different functions $s_1^*(-t)$, …, $s_P^*(-t)$, and the output of each channel is sampled at a rate $1/T$, [2, 3]. The set of samples is given by

$$c_p[n]=\int_{-\infty}^{\infty}y(t)s_p^*(t-nT)dt\ ,\ \ p=1,\dots,P. \qquad (2)$$

The system is said to have a total sampling rate P/T.

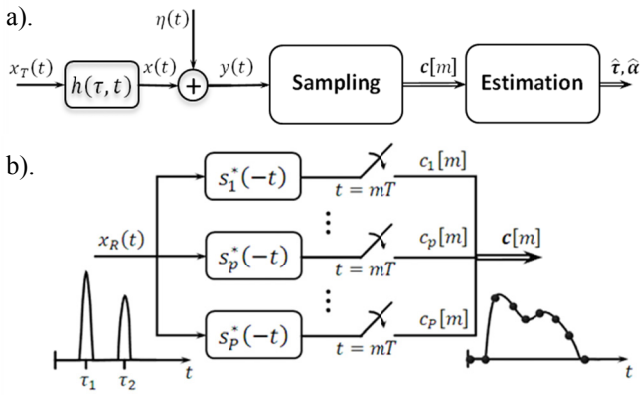

Fig. 1. a). System model; b). Filter-bank sampling block.

Two main multichannel sampling methods were proposed recently in the literature, i.e., the filter-bank method in [2] and the modulator-bank method in [3]. The modulator-bank sampling scheme can be used to treat different FRI signals under the assumption that the pulse $g(t)$ is compactly supported and pulses do not overlap boundaries of interval I_n. In contrast, the filter-bank sampling scheme can accommodate arbitrary pulse shapes $g(t)$, including infinite-length functions. Also, the filter-bank scheme is well suited for sampling long ($N\to\infty$) semi-periodic signals of form (1). For the rest of the paper, the filter-bank sampling is assumed, with the note that similar analysis can be carried out for the modulator-bank scheme.

The filter-bank scheme is illustrated in Fig. 1b. On each branch, the signal is filtered by $s_p^*(-t)$, followed by actual sampling at a rate $1/T$. The signal model is handled easier in the frequency domain. For long observation intervals, $T_0\to\infty$, the discrete-time Fourier transform (DTFT), $C_p(e^{j\omega T})\triangleq\sum_{n\in\mathbb{Z}}c_p[n]e^{-j\omega nT}$, can be applied. With this, (2) becomes

$$C_p(e^{j\omega T})=\frac{1}{T}\sum_{m=-\infty}^{\infty}Y\left(\omega-\frac{2\pi}{T}m\right)S_p^*\left(\omega-\frac{2\pi}{T}m\right), \qquad (3)$$

where $Y(\omega)=X(\omega)+\mathcal{N}(\omega)$ and $X(\omega)$, $Y(\omega)$, $\mathcal{N}(\omega)$, and $S_p^*(\omega)$ denote the Fourier transforms of $x(t)$, $y(t)$, noise $\eta(t)$, and sampling filters $s_p^*(-t)$, respectively. Note that, based on (1), $X(\omega)=G(\omega)\sum_{k=1}^{K}A_k(e^{j\omega T})\,e^{-j\omega\tau_k}$, where $G(\omega)$ is the Fourier transform of $g(t)$.

Focusing, as proposed in [2], on sampling filters with finite support in the frequency domain, e.g., contained in the range $\mathcal{F}=[-P\pi/T\ ,\ P\pi/T]$, (3) becomes

$$C_p(e^{j\omega T})=\frac{1}{T}\sum_{q=1}^{P}S_p^*(\omega+\omega_q)Y(\omega+\omega_q), \qquad (4)$$

where $\omega_q=2\pi(q-1-P/2)/T$. Note that all the

expressions in the frequency domain are $2\pi/T$ periodic and ω is restricted to the interval $[0, 2\pi/T)$.

If $\boldsymbol{c}$ is a column vector collecting $C_p(e^{j\omega T})$ from all the P sampling channels,

$$\boldsymbol{c} = \boldsymbol{S}\boldsymbol{y} = \boldsymbol{S}\boldsymbol{G}\boldsymbol{N}(\boldsymbol{\tau})\boldsymbol{D}\boldsymbol{a} + \boldsymbol{S}\boldsymbol{\eta}, \tag{5}$$

where $\boldsymbol{S}$ is a $P \times P$ matrix of elements $\frac{1}{T}S_p^*(\omega + \omega_q)$, $\boldsymbol{G} = \mathrm{diag}\{G(\omega + \omega_1), \dots G(\omega + \omega_P)\}$, $\boldsymbol{N}(\boldsymbol{\tau})$ is a $P \times K$ matrix of elements $e^{-j\omega_q\tau_k}$, $\boldsymbol{D} = \mathrm{diag}\{e^{-j\omega\tau_1}, \dots e^{-j\omega\tau_K}\}$, $\boldsymbol{a}^T = [A_1(e^{j\omega T}), \dots A_K(e^{j\omega T})]$, $A_k(e^{j\omega T})$ is the DTFT of $a_k[n]$, $\boldsymbol{y}$ is a column vector collecting elements $Y(\omega + \omega_q)$, and $\boldsymbol{\eta}$ is a column vector collecting elements $\mathcal{N}(\omega + \omega_q)$. Although it not explicitly evident in the notation, note the dependence on $e^{j\omega T}$ of the all the arrays in (5) except $\boldsymbol{N}(\boldsymbol{\tau})$. Also note that the unknown time delays τ_K are embedded in $\boldsymbol{N}(\boldsymbol{\tau})$ and $\boldsymbol{D}$, while the unknown amplitudes α_K are in the amplitudes $A_k(e^{j\omega T})$. Matrices $\boldsymbol{S}$ and $\boldsymbol{G}$ are known.

We briefly review the operations performed within the *Estimation* block, as proposed in. First, (5) is normalized by $\boldsymbol{W}^{-1}$, with $\boldsymbol{W} = \boldsymbol{S}\boldsymbol{G}$. Thus, let $\boldsymbol{\mu} = \boldsymbol{W}^{-1}\boldsymbol{c} = \boldsymbol{N}(\boldsymbol{\tau})\boldsymbol{D}\boldsymbol{a} + \boldsymbol{W}^{-1}\boldsymbol{\eta}$. By denoting $\boldsymbol{b} = \boldsymbol{D}\boldsymbol{a}$ and $\overline{\boldsymbol{\eta}} = \boldsymbol{W}^{-1}\boldsymbol{\eta}$ (dependence on $e^{j\omega T}$ continues to be implicit) and taking the inverse DTFT,

$$\boldsymbol{\mu}[n] = \boldsymbol{N}(\boldsymbol{\tau})\boldsymbol{b}[n] + \overline{\boldsymbol{\eta}}[n]. \tag{6}$$

Matrix $\boldsymbol{N}(\boldsymbol{\tau})$ has a Vandermonde structure and thus super-resolution techniques, [5, 6], traditionally used in spectral estimation, can be employed with (6) to estimate the time delays $\boldsymbol{\tau}$, where the number of multipaths K is a priori known, [2]. Once $\boldsymbol{\tau}$ is known, the vector $\boldsymbol{a}$ can be found using the linear relation $\boldsymbol{a} = \boldsymbol{D}^{-1}\boldsymbol{N}^{\dagger}(\boldsymbol{\tau})\boldsymbol{\mu}$, where is the Moore-Penrose pseudo-inverse of $\boldsymbol{N}(\boldsymbol{\tau})$. Further, with knowledge of the sequence $\{x_M[n]\}$, the amplitudes α_k can be determined.

In the absence of noise $\boldsymbol{\eta}$, the filter-bank sampling scheme supports recovery of the signal $x(t)$ only if the number of samples P per interval T is at least $2K$. The number of samples cannot exceed the number at Nyquist rate, $2T\mathcal{B}_g$, where $\mathcal{B}_g$ is the single side bandwidth of the pulse shape (if band-limited), [2, 7]. Combined, these lead to condition $2K \le P \le 2T\mathcal{B}_g$ for the filter-bank scheme to work.

Also note that the values of $\boldsymbol{\mu}[n]$ are obtained in (6) by taking the inverse DTFT of $\boldsymbol{W}^{-1}\boldsymbol{c}$. Thus, the matrix $\boldsymbol{W}$ needs to be stable invertible. One example of sampling filters satisfying this condition is

$$S_p(\omega) = \begin{cases} T, \text{for } \omega \in [\omega_p,\ \omega_p + 2\pi/T] \\ 0, \text{otherwise.} \end{cases} \tag{7}$$

3. CRAMER-RAO BOUND

The performance of an estimate $\widehat{\boldsymbol{\theta}}$ of a vector parameter $\boldsymbol{\theta}$ from a set of measurements is typically measured by its mean squared error (MSE). A lower bound on the MSE is often used instead to gain insight into the factors affecting the MSE. The Cramér-Rao bound (CRB) is a lower bound on the MSE of any unbiased estimate of $\boldsymbol{\theta}$. For the problem at hand, the available measurements are the samples $\boldsymbol{c}$, obtained as (5) by a filter-bank low rate sampling scheme applied to the FRI signal $y(t)$ of (1). Since $\{x_M[n]\}$ in (1) is assumed known, the unknown parameter vector is $\boldsymbol{\theta} = [\tau_1, \dots, \tau_K, \alpha_1^{\mathrm{R}}, \dots, \alpha_K^{\mathrm{R}}, \alpha_1^{\mathrm{I}}, \dots, \alpha_K^{\mathrm{I}}]^{\mathrm{T}}$, where $\alpha_i^{\mathrm{R}} = \mathrm{Re}\{\alpha_i\}$ is the real part of α_i and α_i^{I} is the imaginary part of α_i. The CRB on the MSE of an element θ_i of $\boldsymbol{\theta}$ is given by the i-i element of a matrix $\boldsymbol{C}(\boldsymbol{\theta})$, i.e., $\mathrm{CRB}(\theta_i) = [\boldsymbol{C}(\boldsymbol{\theta})]_{i,i}$. By definition, the matrix $\boldsymbol{C}(\boldsymbol{\theta})$ is the inverse of the Fisher Information Matrix (FIM), whose elements are given by [8],

$$[\boldsymbol{J}(\boldsymbol{\theta})]_{i,j} = \mathbb{E}\left\{\frac{\partial^2 \ln f(\boldsymbol{c};\boldsymbol{\theta})}{\partial\theta_i\,\partial\theta_j}\right\}, \tag{8}$$

where $f(\boldsymbol{c};\boldsymbol{\theta})$ is the probability density function (pdf) of the sample vector $\boldsymbol{c}$, parameterized by $\boldsymbol{\theta}$.

The CRB for the signal reconstruction from low rate samples was discussed in [4]. In contrast, we are concerned here with parameter estimation, rather than estimation of the signal itself. Insight into the performance is developed from closed-form results for a particular setting, as stipulated in Theorem 1 below.

We make the following two assumptions:

(A1) The pulse shape shape $g(t)$ is ideal, in the sense that $G(\omega) = 1$ for $\omega \in [-2\pi\mathcal{B}_g,\ 2\pi\mathcal{B}_g]$ and $G(\omega) = 0$ everywhere else.

(A2) $\Phi_x(\omega) = \left|x(e^{j\omega T})\right|^2$, where $x(e^{j\omega T})$ is the DTFT of the sequence $\{x[n]\}$, and $\Phi_x(\omega)$ is assumed constant and known within the frequency range of interest. With this, we define the signal to noise ratio (SNR) as $\Phi_x(\omega)/\sigma_\eta^2$. Note that if $\{x[n]\}_{n=1}^N$ is a long bipolar sequence, where the $+1$ and -1 symbols are equiprobable, it can be further shown that $\Phi_x = N$, [9].

Theorem 1. Let $\boldsymbol{c}$ in (5) consist of the low rate samples of a semi-periodic stream of pulses in AWGN noise, of form (1). Under assumptions (A1) and (A2), with the choice (7) of the sampling filters, and for a multipath free environment, i.e., $K = 1$, the CRBs for delay and amplitude estimation from low rate samples are:

$$\mathrm{CRB}(\tau_1) = \frac{3}{2\pi^2}\frac{1}{SNR|\alpha_1|^2}\frac{T^2}{P^3}, \tag{9}$$

$$\mathrm{CRB}(\alpha_1) = \frac{1}{SNR}\frac{1}{P}. \tag{10}$$

Proof: See Appendix for a sketch of the proof.

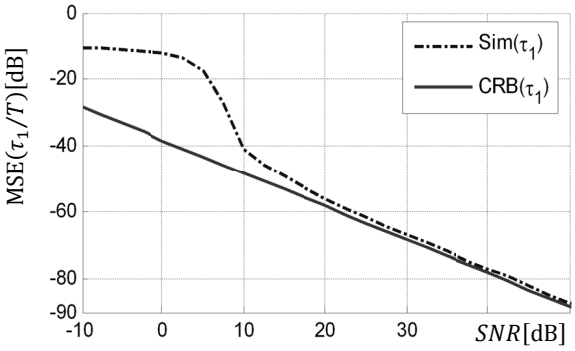

Fig. 2. Accuracy of delay estimation versus SNR.

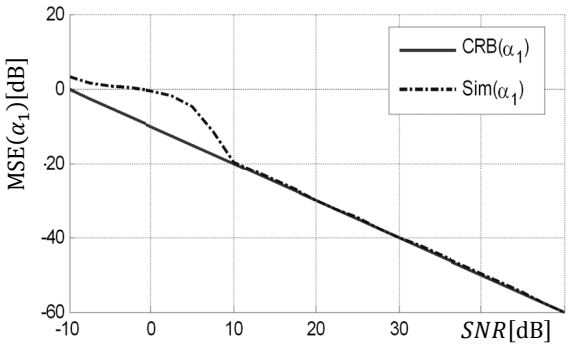

Fig. 3. Accuracy of amplitude estimation versus SNR.

Discussion. The CRB expression (9) shows that the performance of delay estimation improves with the SNR, i.e., the CRB decreases as the SNR increases. The same observation holds for the CRB of amplitude estimation (10). Interestingly, the CRB of delay estimation decreases with the cube of the number of sampling filters, i.e., it is proportional to P^{-3}. This means that increasing the number of sampling filters quickly improves the performance of delay estimation. In contrast, the CRB of amplitude estimation is proportional only to P^{-1}. If we denote $B_P = P/T$, and employ the assumption that $|\alpha_1|^2 = 1$, the CRB can be written as $(3/2\pi^2 B_P^2)(1/B_P\, T\, SNR)$ for delay estimation and $1/B_P T\, SNR$ for amplitude estimation. With these definitions, the expression for the CRB has the same form as the CRB for delay estimation in continuous signals developed in [10], where the term $B_P T\, SNR$ is referred to as postintegration SNR. This is justified by the fact that the product $B_P T$ is the processing gain due to the time bandwidth product of the signal. Thus we observe that the variation with P^3 of the CRB of delay estimation can be split into the effect of bandwidth $P^2$and the effect of processing gain P. In the case of amplitude estimation, the CRB is influenced only by the SNR gain.

4. NUMERICAL EXAMPLES

The MSE of delay estimation (CRB and maximum likelihood simulations) as a function of SNR is shown in Fig. 2 for $N = 100$ symbols, $P = 10$ sampling channels,

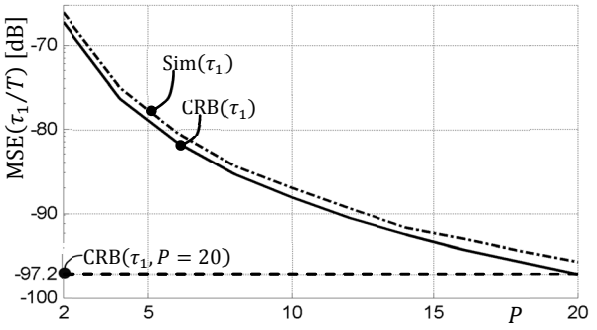

Fig. 4. Delay estimation errors as function of the number of sampling filters.

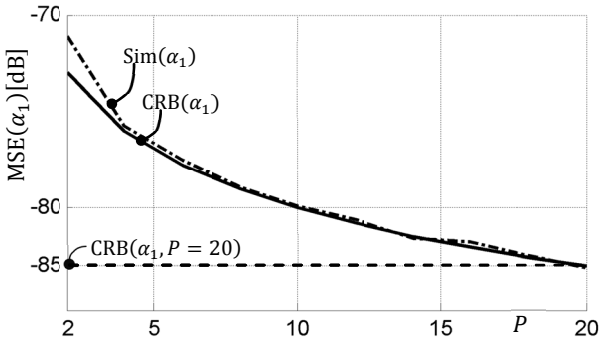

Fig. 5. Amplitude estimation errors as function of the number of sampling filters.

$\alpha_1 = 1$, and $T = 10\mu s$. Results shown are averaged over 1000 runs in which the noise have been chosen randomly (source location was kept fixed). It may be noticed that at high SNR, the MSE from simulations approaches asymptotically the CRB. This confirms that the CRB given by (9) is a tight lower bound. With the logarithmic scaling used in Fig. 2, the CRB decreases linearly with slope -3. In contrast, at low SNR, maximum likelihood estimation experiences a threshold effect, i.e., the MSE increases steeply. This is because, as the SNR decreases, the estimation enters a so called "large-errors" region, where the noise values become dominant over the signal. For the given FRI problem addressed in this work, time delay values are bounded by T andso are the errors, resulting in the plateau region evident at the low end of the SNR scale. In Fig. 3, it is observed that for the same setup as delay estimation, the MSE of amplitude estimation varies linearly with slope -1.

Based on (9) and (10), the performance of delay estimation improves with P^{-3} when P varies from $2K$ to $2TB_g$, while the amplitude estimation performance improves only with P^{-1}. When $P = 2TB_g$, the estimation performance of the filter-bank scheme equals the one of a single filter scheme working at Nyquist rate [1]. This can be observed in Fig. 4, and Fig. 5, where for low rate sampling the simulated MSE and CRB are plotted against the number of sampling filters P. The CRB for Nyquist rate for $TB_g = 10$is the same as the CRB for low rate sampling with $P = 20$.

5. CONCLUSIONS

Performance of time delay and amplitude estimation from low rate samples of pulse trains has been addressed. In particular, the CRB expression for the case of using a filter-bank sampling scheme was developed. With some simplifying assumptions, closed form expressions were determined for multipath free signal. The estimation performance in noise was shown to deteriorate significantly if the number of samples taken is the one indicated by the rate of innovation rather than by the Nyquist rate. Specifically, with the simplifying assumptions considered, the CRB is inverse proportional to the cube of the number of sampling filters for delay estimation and to the number of sampling filters for amplitude estimation.

6. APPENDIX

Due to space considerations, we can provide in this appendix only a sketch of the proof of Theorem 1. We start by expressing the pdf $f(\boldsymbol{c};\boldsymbol{\theta})$ used in (8) in terms of the signal model (1)

$$f(\boldsymbol{c};\boldsymbol{\theta}) = \frac{1}{\det\left(\pi \boldsymbol{K}_{\varepsilon_N}\right)} e^{-(\boldsymbol{c}_N-\tilde{\boldsymbol{\mu}}_N)^{\mathrm{H}}\boldsymbol{K}_{\varepsilon_N}^{-1}(\boldsymbol{c}_N-\tilde{\boldsymbol{\mu}}_N)}, \qquad (11)$$

where $\boldsymbol{c}_N^{\mathrm{T}} = [\boldsymbol{c}^{\mathrm{T}}[1], \dots, \boldsymbol{c}^{\mathrm{T}}[N]\,]$, $\tilde{\boldsymbol{\mu}}_N^{\mathrm{T}} = [\tilde{\boldsymbol{\mu}}^{\mathrm{T}}[1], \dots, \tilde{\boldsymbol{\mu}}^{\mathrm{T}}[N]\,]$, and the observation interval is limited to $[0, NT)$. The matrix $\boldsymbol{K}_{\varepsilon_N}$ denotes the $NP \times NP$ covariance matrix of the noise vector $\boldsymbol{\varepsilon}_N^{\mathrm{T}} = [\boldsymbol{\varepsilon}^{\mathrm{T}}[1], \dots, \boldsymbol{\varepsilon}^{\mathrm{T}}[N]\,]$. Equation (15.52) from [8] is applied to (11), together with the observation that the covariance matrix $\boldsymbol{K}_{\varepsilon_N}$ does not depend on parameter $\boldsymbol{\theta}$ [11], to reduce (8) to

$$[\boldsymbol{J}(\boldsymbol{\theta})]_{i,j} = 2\mathrm{Re}\left\{\frac{\partial \tilde{\boldsymbol{\mu}}_N^{\mathrm{H}}}{\partial \theta_i}\boldsymbol{K}_{\varepsilon_N}^{-1}\frac{\partial \tilde{\boldsymbol{\mu}}_N}{\partial \theta_j}\right\} = \qquad (12)$$

$$= \frac{T}{\pi}\int_{-\pi/T}^{\pi/T} \mathrm{Re}\left\{\frac{\partial(\boldsymbol{\mu}^{\mathrm{H}}\boldsymbol{W}^{\mathrm{H}})}{\partial \theta_i}\left(e^{j\omega T}\right)\boldsymbol{K}_{\varepsilon}^{-1}\frac{\partial(\boldsymbol{W}\boldsymbol{\mu})}{\partial \theta_j}\left(e^{j\omega T}\right)\right\}\mathrm{d}\omega = \qquad (13)$$

$$= \frac{T}{\pi}\int_{-\pi/T}^{\pi/T}\sum_{p=1}^{P}\frac{1}{\sigma_\eta^2}\mathrm{Re}\left\{\frac{\partial \mu_p^*}{\partial \theta_i}(e^{j\omega T})\frac{\partial \mu_p}{\partial \theta_i}(e^{j\omega T})\right\}\mathrm{d}\omega. \qquad (14)$$

Term (13) is obtained from (12) by replacing the data vector $\boldsymbol{c}_N$ by the vector of its Fourier coefficients (obtained by applying the DTFT to $\boldsymbol{c}_N$, when $N \to \infty$) and following a reasoning similar to that in [12]. Matrix $\boldsymbol{K}_\varepsilon$ is a $P \times P$ matrix of elements $[K_\varepsilon(e^{j\omega T})]_{p,q}$ given by the DTFT of the cross-correlation of sequences $\left[\varepsilon_p[1], \dots, \varepsilon_p[N]\right]$ and $\left[\varepsilon_q[1], \dots, \varepsilon_q[N]\right]$. With the choice (7) of sampling filters, $\boldsymbol{K}_\varepsilon$ is $\left(\sigma_\eta^2/T^2\right)\mathrm{diag}\{|S_1(\omega+\omega_1)|^2, \dots |S_P(\omega+\omega_P)|^2\}$. Furthermore, the choice of an ideal pulse shape $g(t)$, in the sense that $G(\omega) = 1$ for $\omega \in \left[-\mathcal{B}_g, \mathcal{B}_g\right]$ and $G(\omega) = 0$ everywhere else, determines that matrix $\boldsymbol{W}(e^{j\omega T})$ is an $P \times P$ identity matrix. This leads to further simplification of (13) to (14).

In (14) we use $\boldsymbol{\theta} = [\tau_1, \dots, \tau_K, \alpha_1^{\mathrm{R}}, \dots, \alpha_K^{\mathrm{R}}, \alpha_1^{\mathrm{I}}, \dots, \alpha_K^{\mathrm{I}}]^{\mathrm{T}}$ and $\mu_p(e^{j\omega T}) = x(e^{j\omega T})\sum_{k=1}^{K}\alpha_k e^{-j(\omega+\omega_p)\tau_k}$ to determine the elements of the FIM. Particularizing it for $K = 1$,

$$\boldsymbol{J}(\boldsymbol{\theta}) = \frac{2P\Phi_x}{\sigma_\eta^2}\left[\begin{array}{c|cc} P^2\pi^2|\alpha_1|^2/3T^2 & 0 & 0 \\ \hline 0 & 1 & 0 \\ 0 & 0 & 1 \end{array}\right]. \qquad (15)$$

With (15), the equations of Theorem 1 can be easily derived. Moreover, it can be shown that for $K \geq 2$, for well separated multipaths, the CRB for the time delay and amplitude of any k^{th} component is also given by Theorem 1.

7. REFFERENCES

[1] T. Blu, P. L. Dragotti, M. Vetterli, P. Marziliano, and L. Coulot, "Sparse Sampling of Signal Innovations," *IEEE Signal Processing Magazine*, vol. 25, pp. 31-40, 2008.

[2] K. Gedalyahu and Y. C. Eldar, "Time-Delay Estimation From Low-Rate Samples: A Union of Subspaces Approach," *IEEE Transactions on Signal Processing*, vol. 58, pp. 3017-3031, 2010.

[3] K. Gedalyahu, R. Tur, and Y. C. Eldar, "Multichannel Sampling of Pulse Streams at the Rate of Innovation," *IEEE Transactions on Signal Processing*, vol. 59, pp. 1491-1504, 2011.

[4] Z. Ben-Haim, T. Michaeli, and Y. C. Eldar, "Performance Bounds and Design Criteria for Estimating Finite Rate of Innovation Signals," *Arxiv preprint arXiv:1009.2221*, 2010.

[5] X. Li and K. Pahlavan, "Super-Resolution TOA Estimation with Diversity for Indoor Geolocation," *IEEE Transactions on Wireless Communications*, vol. 3, pp. 224-234, 2004.

[6] P. Stoica and A. Nehorai, "MUSIC, maximum likelihood, and Cramer-Rao bound," *IEEE Transactions on Acoustics, Speech and Signal Processing*, vol. 37, pp. 720-741, 1989.

[7] W. U. Bajwa, K. Gedalyahu, and Y. C. Eldar, "Identification of Parametric Underspread Linear Systems and Super-Resolution Radar," *IEEE Transactions on Signal Processing*, vol. 59, pp. 2548-2561, 2011.

[8] S. M. Kay, *Fundamentals of Statistical Signal Processing*: *Estimation theory*: Prentice-Hall PTR, 1993.

[9] L. W. Couch II, *Digital and analog communication systems*: Prentice Hall PTR, 2000.

[10] A. Weiss and E. Weinstein, "Fundamental limitations in passive time delay estimation--Part I: Narrow-band systems," *IEEE Transactions on Acoustics, Speech and Signal Processing*, vol. 31, pp. 472-486, 1983.

[11] M. L. Fowler and X. Hu, "Signal models for TDOA/FDOA estimation," *IEEE Transactions on Aerospace and Electronic Systems*, vol. 44, pp. 1543-1550, 2008.

[12] A. Zeira and A. Nehorai, "Frequency domain Cramer-Rao bound for Gaussian processes," *IEEE Transactions on Acoustics, Speech and Signal Processing*, vol. 38, pp. 1063-1066, 1990.